Apoptosis (2016) 21:312–328
DOI 10.1007/s10495-015-1198-x

Anti-tumor activities of luteolin and silibinin in glioblastoma cells: overexpression of miR-7-1-3p augmented luteolin and silibinin to inhibit autophagy and induce apoptosis in glioblastoma in vivo

Mrinmay Chakrabarti[1] · **Swapan K. Ray**[1]

Published online: 16 November 2015

Abstract Glioblastoma is the deadliest brain tumor in humans. High systemic toxicity of conventional chemotherapies prompted the search for natural compounds for controlling glioblastoma. The natural flavonoids luteolin (LUT) and silibinin (SIL) have anti-tumor activities. LUT inhibits autophagy, cell proliferation, metastasis, and angiogenesis and induces apoptosis; while SIL activates caspase-8 cascades to induce apoptosis. However, synergistic anti-tumor effects of LUT and SIL in glioblastoma remain unknown. Overexpression of tumor suppressor microRNA (miR) could enhance the anti-tumor effects of LUT and SIL. Here, we showed that 20 μM LUT and 50 μM SIL worked synergistically for inhibiting growth of two different human glioblastoma U87MG (wild-type p53) and T98G (mutant p53) cell lines and natural combination therapy was more effective than conventional chemotherapy (10 μM BCNU or 100 μM TMZ). Combination of LUT and SIL caused inhibition of growth of glioblastoma cells due to induction of significant amounts of apoptosis and complete inhibition of invasion and migration. Further, combination of LUT and SIL inhibited rapamycin (RAPA)-induced autophagy, a survival mechanism, with suppression of PKCα and promotion of apoptosis through down regulation of iNOS and significant increase in expression of the tumor suppressor miR-7-1-3p in glioblastoma cells. Our in vivo studies confirmed that overexpression of miR-7-1-3p augmented anti-tumor activities of LUT and SIL in RAPA pre-treated both U87MG and T98G tumors. In conclusion, our results clearly demonstrated that overexpression of miR-7-1-3p augmented the anti-tumor activities of LUT and SIL to inhibit autophagy and induce apoptosis for controlling growth of different human glioblastomas in vivo.

Keywords Apoptosis · Autophagy · Glioblastoma · Luteolin · Silibinin · miR-7-1-3p

Abbreviations

LUT	Luteolin
SIL	Silibinin
miR	microRNA
BCNU	Bis-chloroethylnitrosourea
TMZ	Temozolomide
NF-κB	Nuclear transcription factor-kappa B
RAPA	Rapamycin
PKCα	Protein kinase C alpha
XIAP	X-linked inhibitor of apoptosis protein
iNOS	Inducible nitric oxide synthase
PCNA	Proliferating cell nuclear antigen
VEGF	Vascular endothelial growth factor
COX-2	Cyclooxygenase-2
DMSO	Dimethyl sulfoxide
FBS	Fetal bovine serum
MTT	3-(4,5-Dimethylthiazol-2-yl)-2,5-diphenyl tetrazolium bromide
IgG	Immunoglobulin G
ECL	Enhanced chemiluminescence

✉ Swapan K. Ray
swapan.ray@uscmed.sc.edu

[1] Department of Pathology, Microbiology, and Immunology, University of South Carolina School of Medicine, Building 2, Room C11, 6439 Garners Ferry Road, Columbia, SC 29209, USA

Introduction

Glioblastoma is the most common brain tumor that almost always kills the patient within a few months following diagnosis. Glioblastoma is heterogeneous tumor that contains mixed population of cells with different molecular attributes (e.g., wild-type p53, mutant p53). The earlier chemotherapeutic agent bis-chloroethylnitrosourea (BCNU) is no longer a first choice in the treatment of glioblastoma, because BCNU fails to prolong the patient survival significantly. Adult aggressive glioblastoma patients treated with temozolomide (TMZ), which is a relatively newer chemotherapeutic agent, has so far shown a median survival rate of about 14.6 months only [1]. Both BCNU and TMZ are associated with severe side effects and obviously not the magic bullets for glioblastoma. Thus, there is an urgent need to find out the new therapeutic strategy based on natural compounds for inhibition of growth of glioblastomas without significant side effects.

Flavonoids, which are plant-derived secondary metabolites, possess a broad spectrum of pharmacological properties including anti-tumor actions. Many recent investigations reported the conspicuous roles of these plant-derived polyphenols in modulating cancer cell proliferation, differentiation, apoptosis, angiogenesis, metastasis, and multi-drug resistance [2]. Belonging to the flavone group of flavonoids, the anti-tumor effects of luteolin (LUT) include inhibition of autophagy, cell proliferation, angiogenesis, metastasis, and stimulation of apoptotic pathways [3]. Some of LUT molecules may be converted to glucuronides when passing through the intestinal mucosa [4]. An important feature of LUT is its permeability through the blood–brain barrier and thus LUT can be an ideal candidate for application to the therapy of various brain tumors including glioblastoma [5]. LUT treatment of human glioblastoma U87MG cells inhibited interleukin (IL)-1β mediated phosphorylation of inhibitor of nuclear factor-kappa B (NF-κB) p65, extracellular signal-regulated kinase-1/2, and c-Jun amino-terminal kinase [6]. Another recent study suggested that LUT could prevent migration of human glioblastoma U87MG and T98G cells through inhibition of Cdc42 expression and phosphoinositide 3-kinase (PI3K)/Akt activity [7]. LUT also inhibited Akt phosphorylation and survivin expression. Reportedly, LUT inhibits protein kinase C alpha (PKCα) activity, resulting in decrease in the protein level of X-linked inhibitor of apoptosis protein (XIAP). Reduced level of XIAP sensitizes tumor cells to the TNF related apoptosis inducing ligand (TRAIL)-induced apoptosis [8]. LUT also suppresses growth of solid tumor cells such as human skin carcinoma, hepatoma, and ovarian cancer cells [9, 10]. It is expected that LUT can be a promising anti-tumor agent in the treatment of glioblastoma in vivo as well.

Combination therapy with different anti-tumor agents can improve the therapeutic efficacy as this strategy allows the use of sub-lethal doses of drugs to cause more effective destruction of tumor cells without inducing much harm to the healthy normal cells. A natural flavonoid from milk thistle is silibinin (SIL), which has shown exciting anti-tumor effects not only in glioblastoma [11] but also in bladder [12], colon [13], lung [14], skin [15], prostate [16], and hepatocellular [17] carcinoma. Dietary SIL (up to 1 % w/w) strongly retards the urethane-induced lung tumor growth and progression via inhibition of cell proliferation and angiogenesis [18]. Molecular targets of SIL include inhibition of expression of inducible nitric oxide synthase (iNOS), proliferating cell nuclear antigen (PCNA), cyclin D1, vascular endothelial growth factor (VEGF), and cyclooxygenase-2 (COX-2) in lung tumors (18). Also, SIL has been shown to upregulate the tumor suppressor p53 protein and increase its phosphorylation at serine 15 resulting in activation of caspase cascade via Bid cleavage leading to induction of apoptosis [19]. Most in vivo investigations indicated the non-toxic nature and bioavailability of SIL. Earlier studies strongly suggest that LUT and SIL as a combination therapy may produce synergistic anti-tumor effects, which also need to be explored in the treatment of human glioblastoma.

The tumor suppressor microRNA-7 (miR-7) precursor family is an intronic miR that resides in the first intron of the heterogeneous ribonuclear protein K gene on chromosome 9 and is conserved across all species [20]. Recently, miR-7 has been shown to promote differentiation and inhibit epidermal growth factor receptor (EGFR) and Akt signaling pathways in glioblastoma [21, 22]. Overexpression of miR-7 reduced invasion and migration of glioblastoma cells in vitro and inhibited metastasis and tumor growth in animal models [23]. Transfection of miR-7 in glioblastoma cells could modulate expression of 37 differentially expressed genes [24]. These data strongly suggest that miR-7 family may have promising therapeutic potential for controlling growth of glioblastoma. However, molecular mechanisms of miR-7-1-3p remain largely undefined due to limited knowledge of the targets of miR-7-1-3p. Bioinformatics analysis of miRs could be an important strategy for screening and predicting their targets that could be useful for anti-tumor investigations in vitro and in vivo. In our current studies, we have identified that miR-7-1-3p can use XIAP (an anti-apoptotic factor) transcripts as a potential molecular target for its degradation so as to promote induction of apoptosis in glioblastoma for regression of this tumor in vivo.

Our investigation clearly demonstrated that miR-7-1-3p, LUT, and SIL targeted XIAP, PKCα, and iNOS, respectively, to cause significant inhibition of autophagy and induction of apoptosis for controlling the growth of human

glioblastoma U87MG (wild-type p53) and T98G (mutant p53) xenografts. So, overexpression of miR-7-1-3p in combination with LUT and SIL could be a highly promising therapeutic approach against human glioblastomas harboring different p53 status.

Results

Residual cell viability following treatment with LUT and SIL alone and in combination

Results on residual cell viability were generated from U87MG cells (Fig. 1a) and also T98G cells (Fig. 1b) after treatments with different doses (5, 10, or 20 μM) of LUT, (25, 50, or 100 μM) of SIL, or of their combinations. These results were further analyzed by CompuSyn software to determine the combination index (CI) values for both cell lines (Table 1). Based on the CI values, we found that combination of 20 μM LUT and 50 μM SIL most significantly and synergistically reduced cell viability in U87MG (CI = 0.93) and T98G (CI = 0.91) cells (Table 1). Also, combination of 20 μM LUT and 50 μM SIL was found to be more effective than a conventional chemotherapeutic agent such as 10 μM BCNU or 100 μM TMZ for decreasing cell viability in glioblastoma. Based on these observations, we decided to use 20 μM LUT and 50 μM SIL in U87MG and T98G cells to carry out subsequent experiments.

Induction of morphological and biochemical features of apoptosis

The morphological and biochemical features of apoptosis after single or combination treatments of cells with LUT and SIL were analyzed using, respectively, in situ Wright staining and Annexin V staining followed by flow cytometry (Fig. 2). In situ Wright staining confirmed the characteristic morphological features like shrinkage of cell volume, chromatin condensation, and membrane-bound apoptotic bodies in apoptotic cells (Fig. 2a). Most of the apoptotic cells (some shown with arrows) were observed following treatment with combination of 20 μM LUT and 50 μM SIL in both glioblastoma cell lines. Following treatment with this combination, results obtained from Annexin V staining followed by flow cytometry also showed the highest apoptotic population (Fig. 2b). Accumulation of Annexin V positive cells in A4 quadrant indicated appearance of a prominent biochemical feature of apoptosis after the treatments (Fig. 2b). Based on the in situ Wright staining and Annexin V staining of cells, we quantified the percentages of

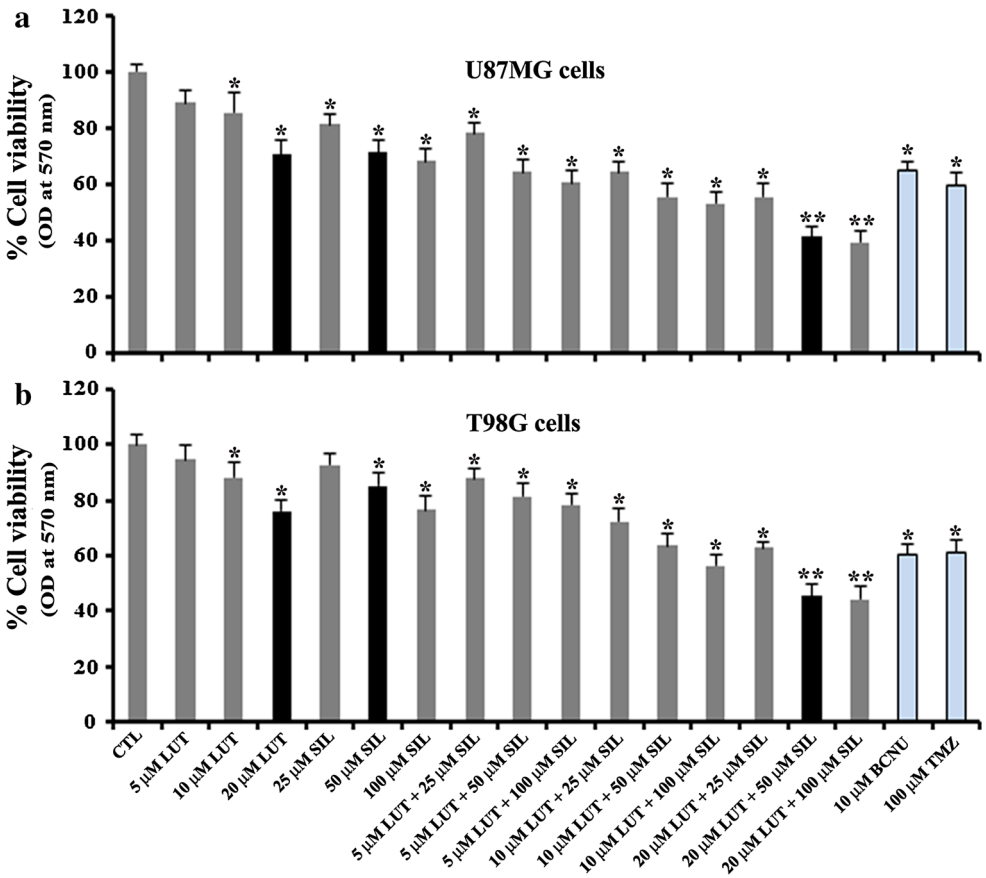

Fig. 1 Determination of changes in residual cell viability in human glioblastoma U87MG (**a**) and T98G (**b**) cells after treatments with different doses of LUT (5, 10, and 20 μM), SIL (25, 50, and 100 μM), and their combinations for 24 h. Cells as untreated control (CTL), 10 μM BCNU, and 100 μM TMZ were also included in the experiments. After the treatments, changes in cell viability were determined by the MTT assay. All experiments were conducted in triplicates ($n = 3$) and the results were analyzed for statistical significance. Difference between the untreated CTL group and a drug treatment group was considered significant at $*p < 0.05$ or $**p < 0.01$

Table 1 Combination index (CI) of LUT and SIL in human glioblastoma U87MG and T98G cells

U87MG cells			T98G cells		
LUT (μM)	SIL (μM)	CI values	LUT (μM)	SIL (μM)	CI values
5	25	1.322	5	25	1.293
5	50	1.234	5	50	1.264
5	100	1.221	5	100	1.119
10	25	1.083	10	25	1.017
10	50	1.013	10	50	1.063
10	100	0.942	10	100	0.983
20	25	1.014	20	25	1.162
20	**50**	**0.932**	**20**	**50**	**0.914**
20	100	1.076	20	100	0.952

The CI values were determined for U87MG and T98G cells after treatment with different doses (μM) of LUT and SIL (5 + 25, 5 + 50, 5 + 100, 10 + 25, 10 + 50, 10 + 100, 20 + 25, 20 + 50, and 20 + 100). Conventionally, CI > 1 indicates antagonistic effect, CI = 1 indicates additive effect, and CI < 1 indicates synergistic effect. The lowest CI values (shown in *bold*) indicate the highest synergistic effect of the combination of two agents

apoptosis in glioblastoma U87MG and T98G cells after all treatments (Fig. 2c). Compared with control or single treatment of U87MG and T98G cells, treatment with combination of 20 μM LUT and 50 μM SIL most effectively induced apoptotic death in both glioblastoma cells.

Treatment with combination of LUT and SIL almost completely blocked cell invasion

We performed matrigel invasion assay to investigate the anti-tumor effects of LUT and SIL on the invasive property of glioblastoma U87MG and T98G cells (Fig. 3a). The staining of cells that invaded through the polycarbonate membrane clearly indicated significant reduction in number of the invaded glioblastoma cells following treatment with LUT or/and SIL, when compared with the untreated control cells. The treatment with combination of LUT and SIL almost completely blocked tumor cell invasion, when compared with either treatment alone.

Treatment with combination of LUT and SIL most significantly inhibited in vitro angiogenic network formation

We examined the in vitro angiogenic network formation in co-culture of human microvascular endothelial (HME) cells and human glioblastoma cells following treatment with LUT and SIL (Fig. 3b). The co-culture of HME cells and U87MG cells or T98G cells showed capillary-like network formation ability of HME cells. Such network formation ability of HME cells was significantly reduced in co-culture with glioblastoma cells after monotherapy with LUT (35 %) or SIL (40 %), and almost completely inhibited (93 %) after combination therapy (Fig. 3b).

Treatment with combination of LUT and SIL inhibited cell migration from spheroids

We examined cell migration from U87MG and T98G spheroids following treatment with LUT or/and SIL (Fig. 3c). When compared with the untreated control, single treatment with LUT or SIL did significantly inhibit cell migration from the spheroids, but treatment with combination of LUT and SIL completely inhibited cell migration from the spheroids.

Treatment with combination of LUT and SIL inhibited rapamycin (RAPA)-induced autophagy

In cell culture medium, RAPA imitates starvation that induces autophagy, which is a potential survival mechanism in tumor cells under a stress condition [25, 26]. We investigated whether combination of LUT and SIL could block the survival strategy like autophagy in both glioblastoma U87MG and T98G cells (Fig. 4). Cells were not treated with anything or pre-treated with 200 nM RAPA for 24 h and then exposed to LUT or/and SIL for another 24 h. Flow cytometric analysis of the acridine orange (AO) stained cells revealed that untreated control cells maintained a very low basal level of autophagy (3–5 %), but RAPA pre-treatment induced more than 40 % autophagy in both U87MG and T98G cells (Fig. 4a). We found that LUT was more potent than SIL in inhibiting autophagy in RAPA pre-treated glioblastoma cells. But combination of LUT and SIL very dramatically blocked occurrence of autophagic populations in both U87MG and T98G cells (Fig. 4a). We analyzed the flow cytometric data from six independent experiments to determine autophagic populations and presented the results in bar diagrams (Fig. 4b).

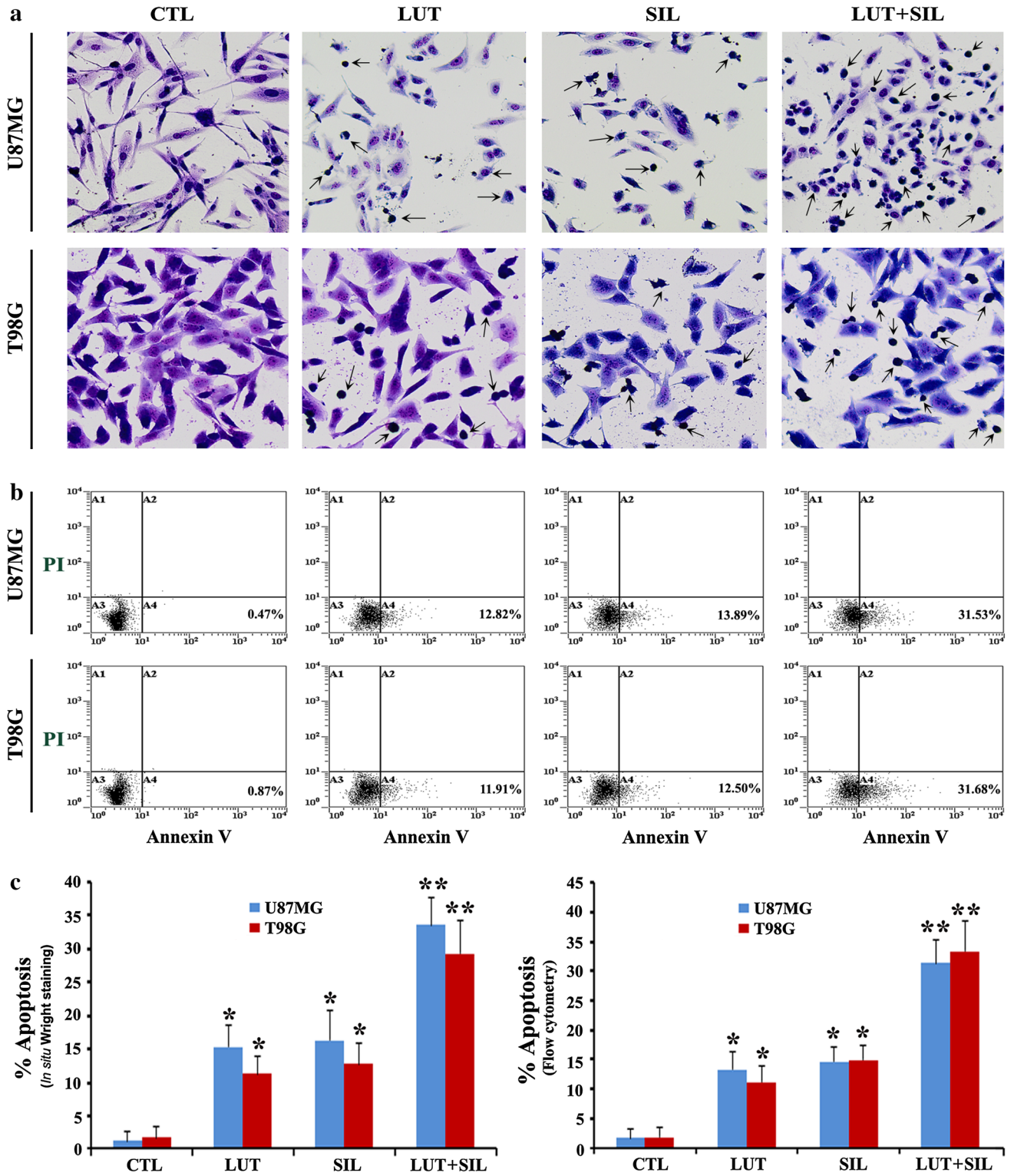

Fig. 2 Determination of induction of morphological and biochemical features of apoptosis in glioblastoma cells following treatments. Treatments for 24 h: untreated control (CTL), 20 μM LUT, 50 μM SIL, and combination of both agents. **a** In situ Wright staining to investigate the morphological features of apoptosis. Some of the apoptotic cells were shown with arrows. **b** Annexin V-FITC/PI double staining followed by flow cytometric analysis of apoptotic populations after treatments. Single treatment with LUT or SIL and treatment with combination of both agents accumulated significant population of cells in A4 quadrant, indicating induction of an early biochemical feature of apoptotic death. **c** Quantitative analysis of apoptotic population based on in situ Wright staining and Annexin V-FITC staining. Significant difference between CTL and a treatment was indicated by $*p < 0.05$ or $**p < 0.01$

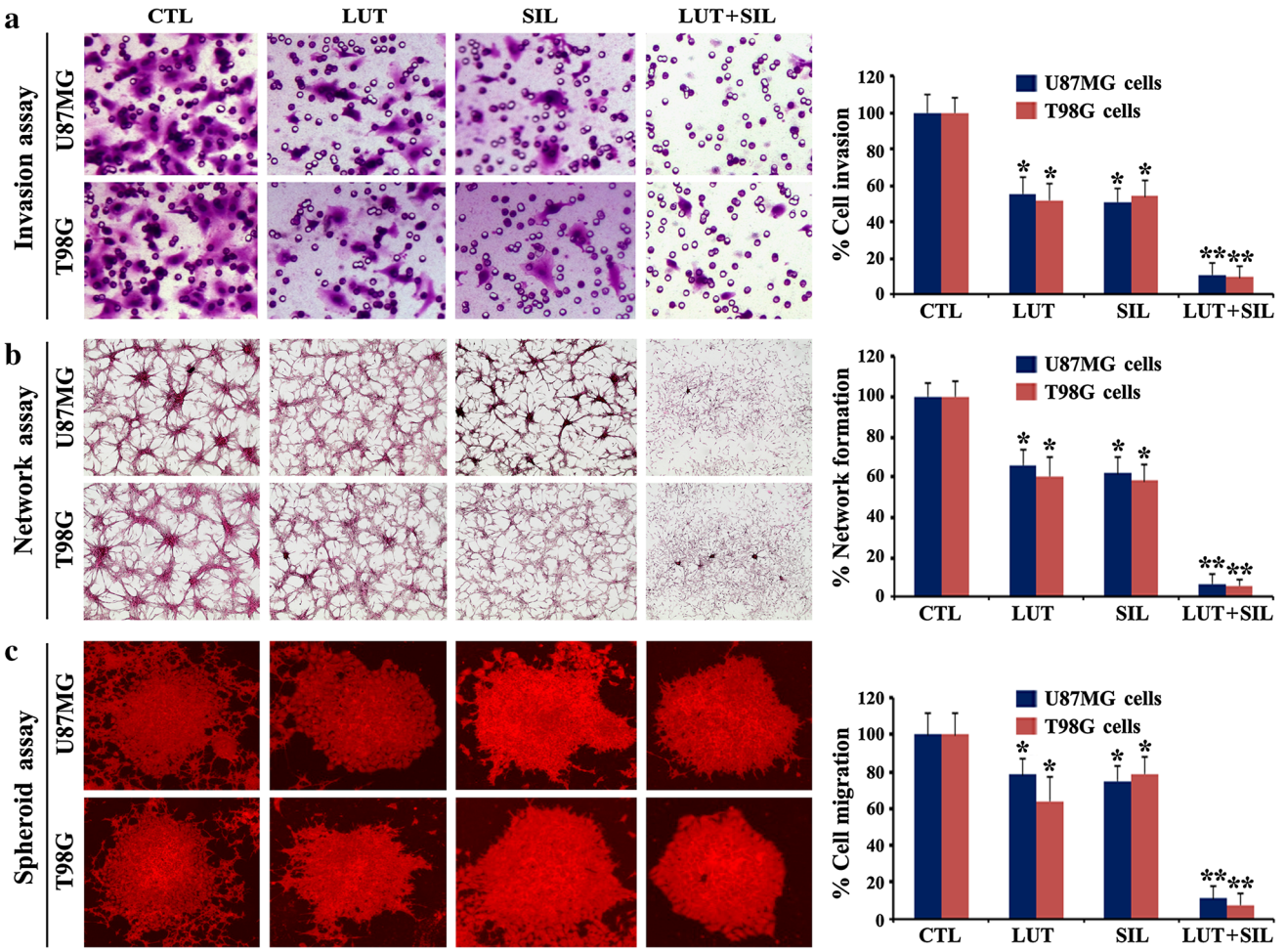

Fig. 3 Invasion, network formation, and spheroid assays with glioblastoma cells following treatments. **a** Representative results of cell invasion assay and quantitative analysis for percentage of cell invasion. Treatments for 48 h: untreated control (CTL), 20 μM LUT, 50 μM SIL, and both agents together. Invasion assays were carried out in 12-well transwell inserts of polycarbonate filters with 12.0 μm pores and coated with 200 μl of 0.1 % matrigel. After 48 h of incubation, the membranes were collected and stained. A significant reduction in the number of invaded cells was an indication of decrease in cell invasion. **b** Evaluation of network formation ability of HME cells in co-culture with glioblastoma U87MG or T98G cells. Treatments of glioblastoma cells for 24 h: untreated CTL, 20 μM LUT, 50 μM SIL, and both agents together. Then, HME cells were co-cultured with glioblastoma cells. The co-cultures were terminated at 72 h and immunocytochemically stained for expression of the von Willebrand factor VIII in HME cells and in vitro networks were quantified. **c** Determination of migration of U87MG and T98G cells from their spheroids after treatments. Treatments of glioblastoma cells for 48 h: untreated CTL, 20 μM LUT, 50 μM SIL, and both agents together. Spheroids were prepared using U87MG or T98G cells following stable expression of a red fluorescent protein, transferred to a 24-well plate, and allowed to migrate from spheroids for 24 h. The cell migrations from the spheroids were observed under a fluorescent microscope and photographs were taken. All quantitative data were shown as mean ± SEM of independent experiments ($n = 6$). Significant difference between CTL group and a treatment group was indicated by $^{*}p < 0.05$ or $^{**}p < 0.01$

Combination of LUT and SIL altered expression of signaling molecules involved in autophagy and apoptosis

We performed Western blotting to explore the molecular events involved in inhibition of RAPA-induced autophagy and induction of apoptosis in U87MG and T98G cells after treatment with LUT and SIL alone and in combination (Fig. 5). Our results showed that LUT alone and in combination with SIL could inhibit expression of the classical PKCα resulting in suppression of RAPA-induced autophagy. Combination of LUT and SIL suppressed the autophagy inducing protein Beclin-1 in both cell lines, suggesting inhibition of autophagic activity. In course of autophagy, microtubule associated protein light chain 3 B (LC3B) is post-translationally converted to LC3B I form, which undergoes lipidation and converted into the autophagosome membrane bound LC3B II form. Our Western blotting showed that treatment with combination of LUT and SIL down regulated expression of both LC3B I

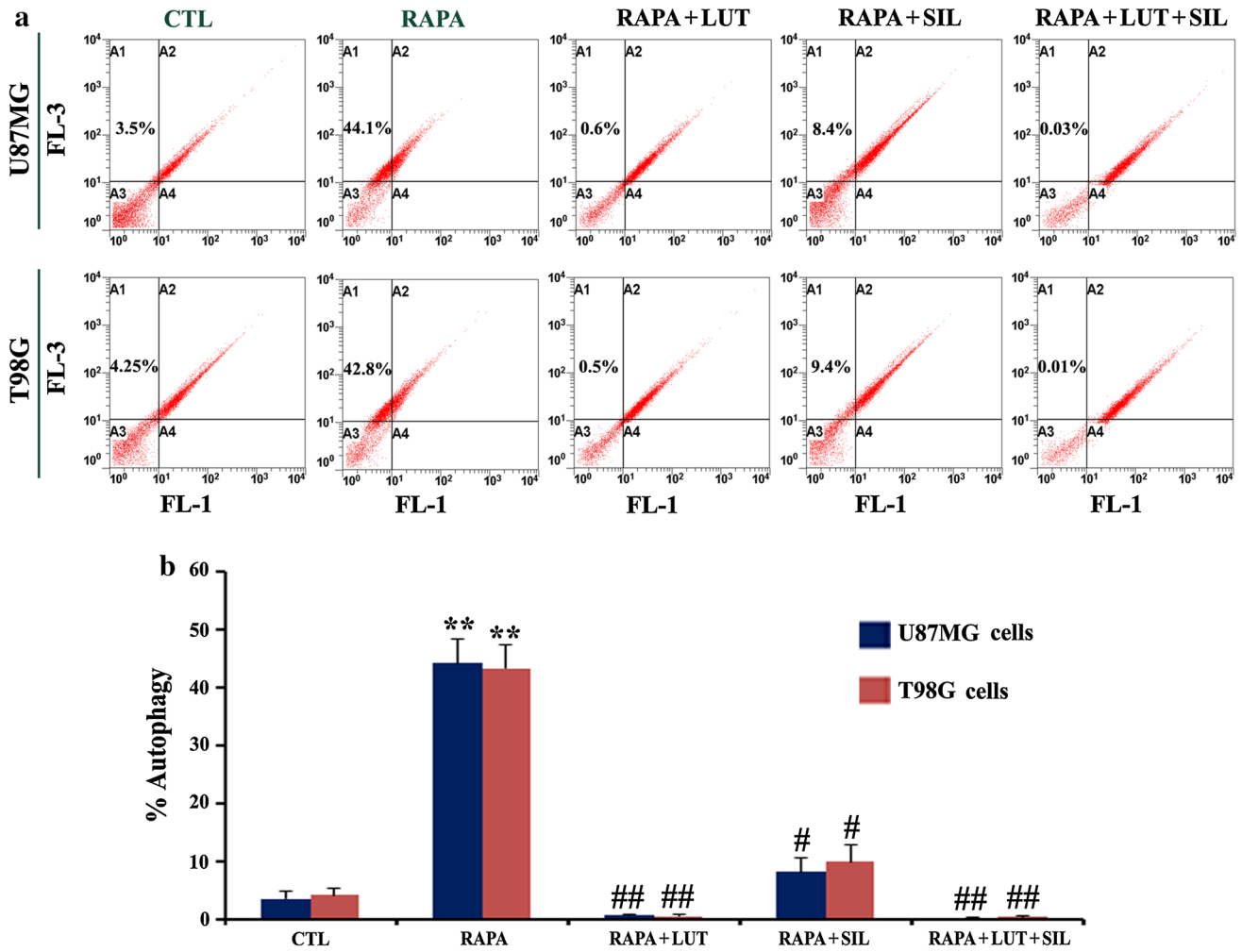

Fig. 4 Evaluation of therapeutic potential of LUT and SIL for inhibition of autophagy in RAPA pre-treated glioblastoma U87MG and T98G cells. Here, a group of each glioblastoma cells without any treatment was used as the untreated control (CTL). Also, glioblastoma cells were pre-treated with 200 nM RAPA for 24 h and then treated with LUT or/and SIL for another 24 h followed by incubation with AO (1 μg/ml) for 15 min. All experiments were performed in triplicates. **a** Detection of AVO in autophagic cells by flow cytometry. **b** Determination of percentages of autophagic populations after AO staining. Significant difference between CTL group and a treatment group was indicated by $^{**}p < 0.01$ whereas significant difference between RAPA pre-treatment group and flavonoid (LUT or/and SIL) treatment group was indicated by $^{\#}p < 0.05$ or $^{\#\#}p < 0.01$

and LC3B II forms, indicating inhibition of RAPA-induced autophagic activity (Fig. 5).

Then, we investigated expression of molecules involved in extrinsic and intrinsic pathways of apoptosis in U87MG and T98G cells following all treatments (Fig. 5). Inhibition of expression of PKCα was correlated with decrease in expression of the anti-apoptotic XIAP protein leading to induction of apoptosis in glioblastoma cells. Also, inhibition of expression of iNOS occurred in both glioblastoma cells following single treatment with SIL and combination treatment with LUT and SIL. Suppression of NO synthesis by iNOS could augment activation of caspase-8 that could trigger induction of extrinsic pathway of apoptosis. Further, combination of LUT and SIL could cause increase in expression of Bax (pro-apoptotic protein) and decrease in expression of Bcl-2 (anti-apoptotic protein), which could thereby result in an increase in Bax:Bcl-2 ratio for induction of intrinsic pathway of apoptosis in both glioblastoma cell lines. Our results confirmed that combination of LUT and SIL indeed induced intrinsic pathway of apoptosis for activation of caspase-9, which in turn activated caspase-3 for completion of apoptosis in glioblastoma U87MG and T98G cells.

Combination of LUT and SIL most effectively increased expression of miR-7-1-3p

Results from our real-time quantitative reverse transcription-polymerase chain reaction (qRT-PCR) experiments

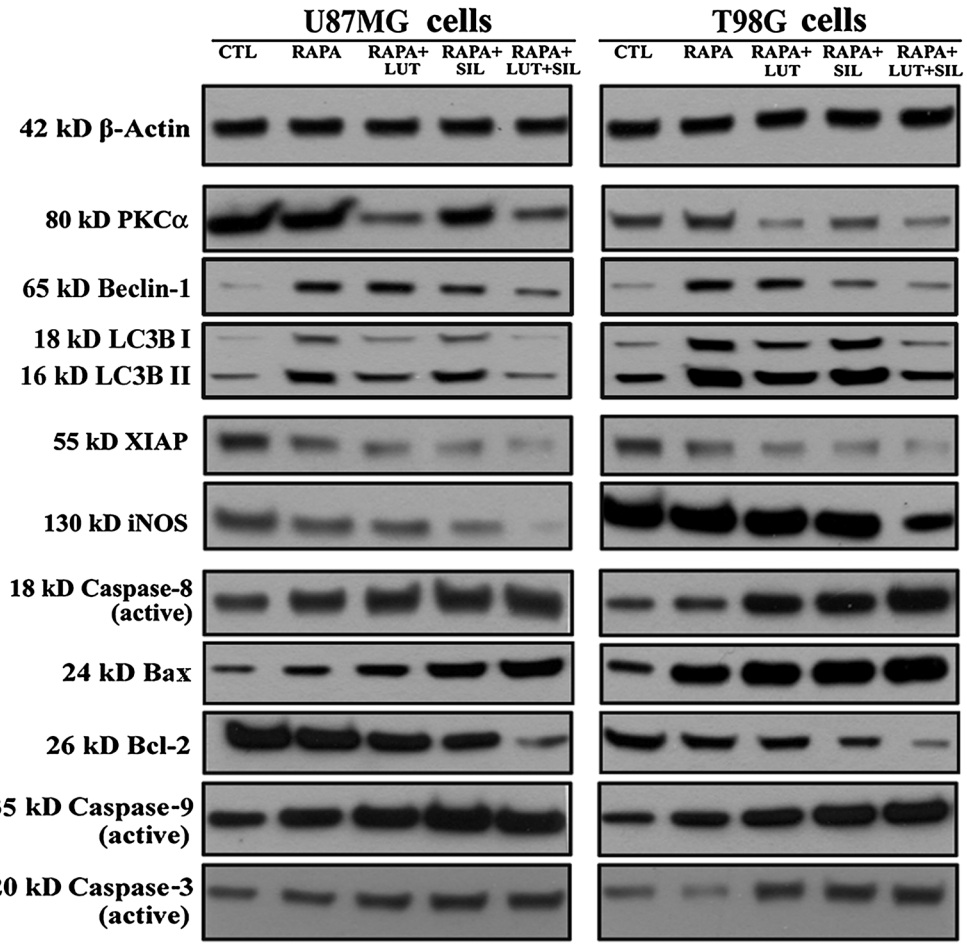

Fig. 5 Western blotting to examine changes in expression of molecular components of autophagy and apoptosis following treatments of glioblastoma U87MG and T98G cells. Treatments: untreated control (CTL), 200 nM RAPA for 24 h, 200 nM RAPA for 24 h + 20 μM LUT for another 24 h, 200 nM RAPA for 24 h + 50 μM SIL for another 24 h, and 200 nM RAPA for 24 h + both 20 μM LUT and 50 μM SIL for another 24 h. Representative Western blots show inhibition of autophagy signaling molecules and activation of the caspases in extrinsic and intrinsic pathways of apoptosis. Expression of β-actin was used as a loading standard. All experiments were conducted in triplicates

showed the levels of expression of three potent tumor suppressor miRs (miR-7-1-3p, miR-9, and miR-181a) in glioblastoma U87MG and T98G cells pre-treated with RAPA and then treated with LUT or/and SIL (Fig. 6). All these tumor suppressor miRs (miR-7-1-3p, miR-9, and miR-181a) were upregulated due to treatment with LUT or/and SIL when compared with only RAPA pre-treated cells (Fig. 6). The relative changes in expression of these miRs were most significant when cells were treated with LUT alone or in combination with SIL. The most dramatic changes were observed in the relative expression of miR-7-1-3p (two-fold increase) in both cell lines. So, we hypothesized that overexpression of miR-7-1-3p could further enhance the anti-tumor efficacy of the combination of LUT and SIL for the highest inhibition of autophagy and augmentation of apoptosis. Subsequently, we performed in vivo experiments to test this hypothesis.

Overexpression of miR-7-1-3p enhanced efficacy of LUT and SIL for regression of tumors

Our in vivo studies showed that ectopic overexpression of miR-7-1-3p and treatment with combination of LUT and SIL very effectively reduced the growth of RAPA pre-treated U87MG and T98G xenografts in athymic nude mice (Fig. 7a). We did not observe any difference in tumor growth among untreated control mice, RAPA pre-treated mice (data not shown), and RAPA pre-treated and miR-7-1-3p mimics injected mice carrying U87MG and T98G xenografts. Compared with untreated controls and RAPA pre-treated tumors with overexpression of anti-miR-7-1-3p, overexpression of miR-7-1-3p significantly enhanced efficacy of combination of LUT and SIL for regression of the RAPA pre-treated U87MG and T98G tumors (Fig. 7b). Following the treatments, hematoxylin and eosin (H&E)

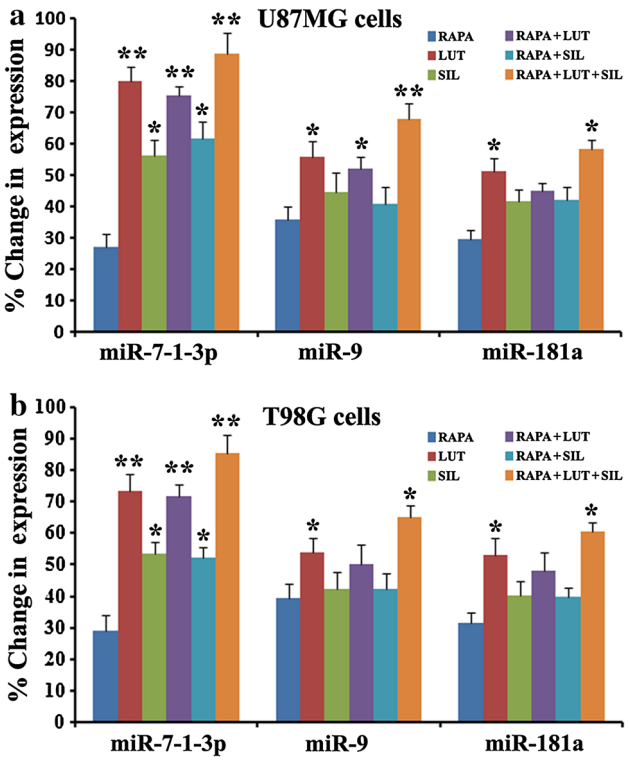

Fig. 6 Real-time qRT-PCR analyses for examination of expression of miR-7-1-3p, miR-9, and miR-181a after treatments with LUT or/and SIL in RAPA pre-treated U87MG (**a**) and T98G (**b**) cells. Treatments: 200 nM RAPA for 24 h, 20 μM LUT for 24 h, 50 μM SIL for 24 h, 200 nM RAPA for 24 h + 20 μM LUT for another 24 h, 200 nM RAPA for 24 h + 50 μM SIL for another 24 h, and 200 nM RAPA for 24 h + both 20 μM LUT and 50 μM SIL for another 24 h. Real-time qRT-PCR analysis was performed for relative expression of each targeted miR after normalizing with expression of U6 RNA (internal standard) in glioblastoma U87MG and T98G cells. Significant difference between RAPA pre-treatment group and another treatment group was indicated by $*p < 0.05$ or $**p < 0.01$

staining of tumor sections and histopathological examinations showed that untreated control tumors maintained characteristic growth; while overexpression of miR-7-1-3p, treatment with LUT alone, or SIL alone induced morphological features of apoptotic death to some extent; but overexpression of miR-7-1-3p and combination therapy with LUT and SIL most dramatically increased apoptotic death in RAPA pre-treated U87MG and T98G xenografts (Fig. 7c).

Overexpression of miR-7-1-3p degraded XIAP and potentiated LUT and SIL to inhibit autophagy and induce apoptosis in glioblastoma xenografts.

We used Western blotting to reveal different molecular signaling pathways for inhibition of autophagy and induction of apoptosis following overexpression of miR-7-1-3p and treatment with LUT or/and SIL in RAPA pre-treated U87MG and T98G xenografts (Fig. 8). Untreated control tumors and RAPA pre-treated tumors with overexpression of anti-miR-7-1-3p showed almost similar expression of different molecules of autophagic and apoptotic pathways. Treatment with LUT and SIL alone prominently inhibited expression of PKCα (autophagy inducer) and iNOS (apoptosis inhibitor), respectively, in the RAPA pre-treated glioblastoma U87MG and T98G xenografts. Overexpression of miR-7-1-3p not only augmented LUT for decreasing PKCα leading to induction of auotphagy inhibitory markers such as mammalian target of rapamycin (mTOR, an autophagy inhibitor) and sequestosome 1 (SQSTM1) also called p62 (an autophagy substrate) and degradation of the anti-apoptotic XIAP protein, but also potentiated SIL for inhibiting iNOS for promotion of extrinsic pathway (caspase-8 activation and production of tBid) of apoptosis as well as of intrinsic pathway (increase in Bax and decrease in Bcl-2 leading to ultimate activation of caspase-3) of apoptosis in the RAPA pre-treated glioblastoma U87MG and T98G xenografts. Thus, our molecular studies in glioblastoma xenografts showed that overexpression of miR-7-1-3p augmented combination of LUT and SIL for controlling in vivo growth of human glioblastoma harboring wild-type p53 or mutant p53.

Materials and methods

Cell culture and treatments

Human glioblastoma U87MG (wild-type p53) and T98G (mutant p53) cell lines were purchased from American Type Culture Collection (Manassas, VA, USA). Both glioblastoma cell lines were grown at 37 °C in DMEM medium supplemented with 10 % fetal bovine serum (FBS) and 1 % penicillin and 1 % streptomycin (GIBCO/BRL, Grand Island, NY, USA) in a fully-humidified incubator containing 5 % CO_2. The DMEM medium and FBS were procured from Mediatech (Atlanta Biologicals, Atlanta, GA, USA). LUT and SIL (Sigma Chemical, St. Louis, MO, USA) were dissolved in dimethyl sulfoxide (DMSO) and stored at −20 °C. In all experiments, control cultures contained the same volume of DMSO that was used with LUT and SIL for 24 h. Following all treatments, cells were used for determination of residual cell viability, morphological and biochemical features of apoptosis, flow cytometry, invasion assay, network formation assay, spheroid assay, and alterations in RAPA-induced autophagy and expression of different tumor suppressor miRs.

Determination of cell viability using the 3-(4,5-dimethylthiazol-2-yl)-2,5-diphenyl tetrazolium bromide (MTT) assay

Residual cell viability in U87MG and T98G cells was determined by the MTT assay following treatments with

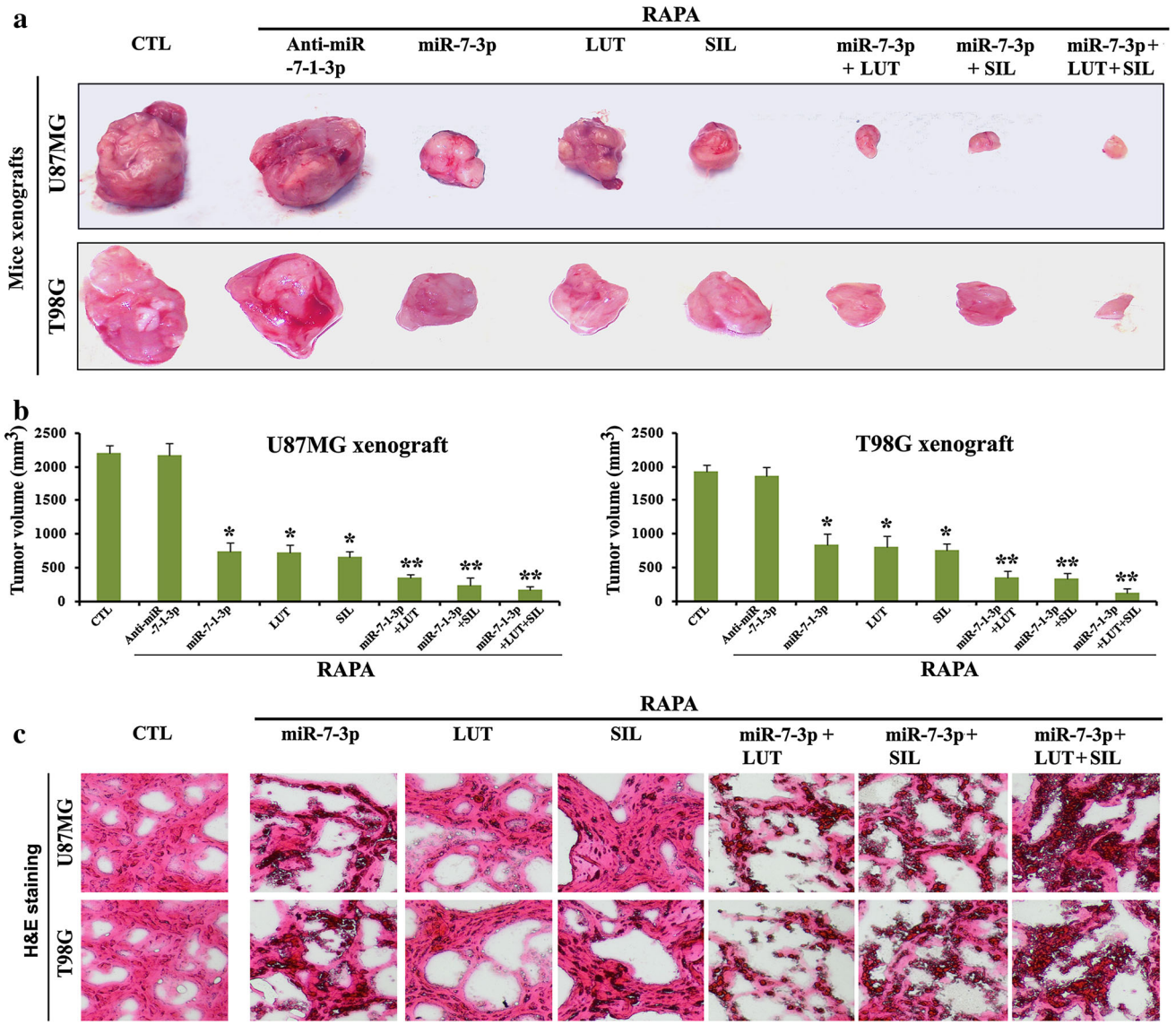

Fig. 7 Regression of U87MG and T98G tumors in athymic nude mice and histopathological changes in tumor sections. Mice bearing xenografts were treated for 3 weeks. After 1 week of tumor inoculation, animals were untreated or daily pre-treated with RAPA (2 mg/kg body weight) for 7 days. One week after RAPA pre-treatment, mice were randomly assigned to eight separate experimental groups for these treatments: untreated control (CTL), 50 µg of anti-miR-7-1-3p each alternate day, 50 µg of miR-7-1-3p each alternate day, LUT (10 mg/kg/day), SIL (200 mg/kg/day), 50 µg of miR-7-1-3p each alternate day + LUT (10 mg/kg/day), 50 µg of miR-7-1-3p each alternate day + SIL (200 mg/kg/day), and 50 µg of miR-7-1-3p each alternate day + LUT (10 mg/kg/day) + SIL (200 mg/kg/day). We used 6 athymic nude mice in each treatment group. After all the therapeutic treatments for 7 days, mice were sacrificed under anesthesia, tumors were surgically removed, and tumor volumes were calculated. **a** Surgical removal of U87MG and T98G xenografts from nude mice after different treatments. **b** Determination of regression of tumor volumes after different therapeutic treatments. Significant difference between CTL group and a treatment group was indicated by $*p < 0.05$ or $**p < 0.01$. **c** Evaluation of histopathological changes in tumors after the treatments

different doses of LUT, SIL, or their combinations. Briefly, the cells were seeded into 96-well micro-culture plates at 1×10^4 cells/well and allowed to attach overnight. Next day, complete growth medium was removed with fresh DMEM medium supplemented with 2 % FBS and then cells were treated with 5, 10, and 20 µM LUT or 25, 50, and 100 µM SIL, or their combinations for 24 h. Two positive treatment control sets were also investigated where cells were treated with 10 µM BCNU or 100 µM TMZ and incubated for 24 h to compare the efficacy of flavonoids with standard chemotherapeutic drugs. After incubation, cells were washed and treated according to the manufacturer's protocol (Chemicon International, Temecula, CA, USA). Briefly, glioblastoma cells were washed twice in

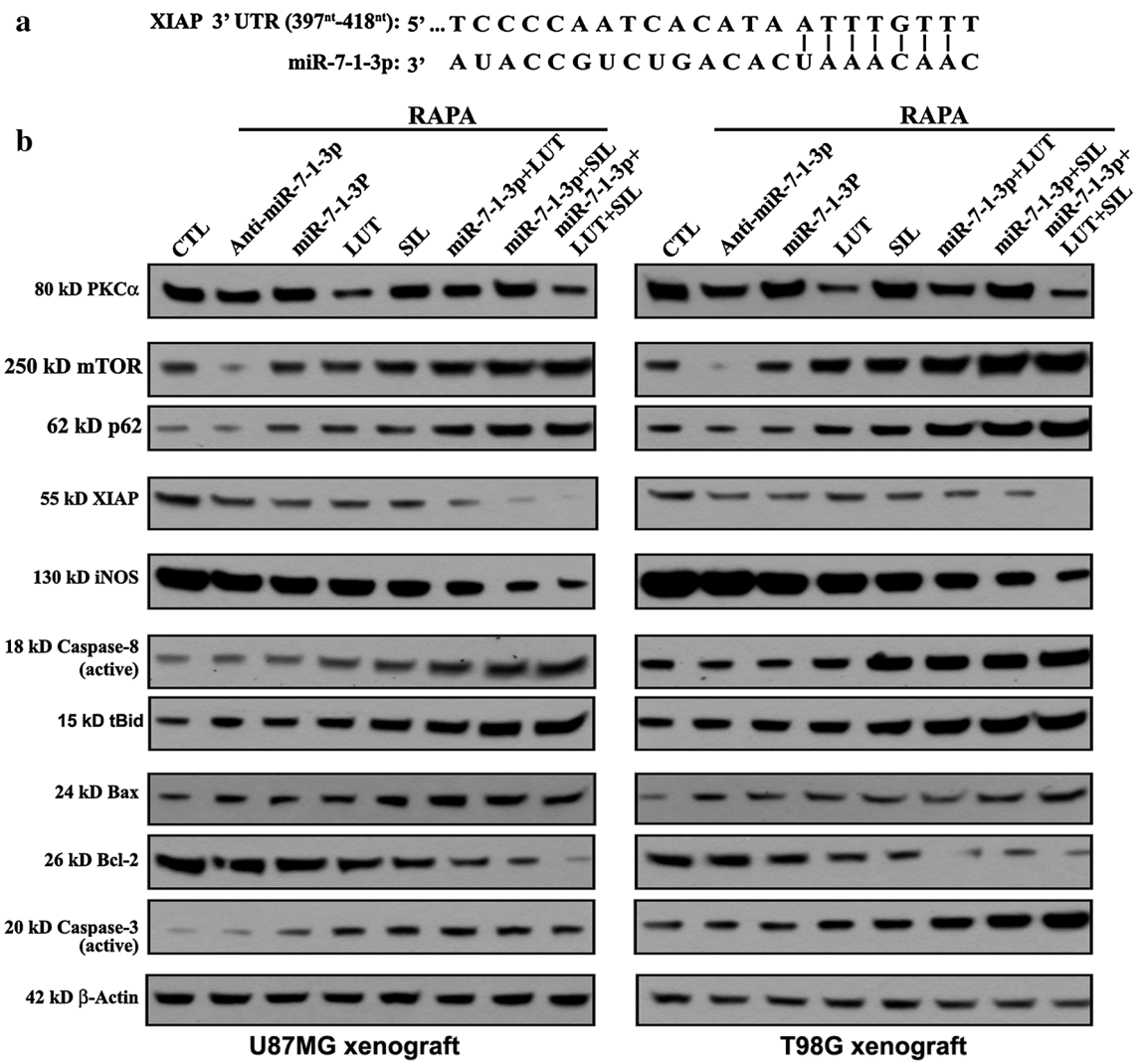

Fig. 8 Use of miRDB for miR-7-1-3p target prediction and Western blotting for examination of changes in expression of autophagy and apoptosis signaling molecules in U87MG and T98G xenografts. **a** Bioinformatic analysis using miRDB indicated that XIAP mRNA could be a potential molecular target of miR-7-1-3p. **b** Nude mice bearing U87MG and T98G xenografts were treated for 3 weeks (as described in Fig. 7 legend). After all therapeutic treatments, nude mice were sacrificed under anesthesia, tumors were surgically removed, and protein samples were isolated for Western blotting. Representative Western blots show inhibition of autophagy and activation of the caspases for induction of both the extrinsic and intrinsic pathways of apoptosis. Expression of β-actin was used as a loading standard. All experiments were conducted in triplicates

phosphate-buffered saline (PBS, pH 7.4), treated with MTT (0.2 mg/ml), and further incubated for 3 h. Then, DMSO was added to dissolve MTT formazan crystals and absorbance or optical density (OD) was measured using a multi-well scanning spectrophotometer at 570 nm. Residual cell viability in different treatments was calculated with the OD values obtained at 570 nm. The CI values at different doses of LUT and SIL were determined from the MTT data using CompuSyn software (ComboSyn, Paramus, NJ, USA). For determination of CI values, we used 3 different doses of LUT and SIL via two-fold dilutions of each drug. All in vitro MTT assays were performed on the same day under similar standardized conditions and in triplicate and only the average effect values for each concentration were used for the dose-effect data entries into the computer for automated analysis [27]. The manual inputs of experimental data took 15 min and computerized simulation results were obtained within 1–2 s. Conventionally, CI $>$ 1 indicates antagonism, CI $=$ 1 indicates additive effect, and CI $<$ 1 indicates synergism of the drugs used in combination treatments.

Morphological and biochemical tests for detection of induction of apoptosis

Cells were grown in 6-well plates and treated with LUT, SIL, or their combinations and incubated for 24 h, as described

above. Then, cells were centrifuged at 2000 rpm for 6 min and washed twice with PBS before being fixed with 95 % ethanol. For detection of the morphological features of apoptosis, in situ Wright staining was performed using HEMA 3 stain kit following manufacturer's protocol (Fisher Scientific, Kalamazoo, MI, USA). The morphological features of the apoptotic cells were observed under the light microscope and photographed. Apoptotic cells ($n = 300$) were counted randomly in different fields and apoptotic population was quantified. The morphological features of apoptotic cells included chromatin condensation, cell shrinkage, or/and membrane-bound apoptotic body formation.

An early biochemical feature of apoptosis, the externalization of cell membrane phosphatidylserine, was detected by Annexin V staining followed by flow cytometry. Briefly, cells were harvested at the completion of all treatments as described above and washed with PBS and fixed with 70 % ethanol for 15 min on ice. Subsequently, cells were centrifuged at a low rpm to obtain pellets and residual ethanol was aspirated. All RNA molecules in the cells were then digested with DNase-free RNase A (2 mg/ml) for 30 min at 37 °C. For Annexin V-fluorescein isothiocyanate (FITC)/propidium iodide (PI) double staining, cells were processed as per the manufacturer's instructions (BD Bioscience, San Jose, CA, USA) and then analyzed on the Epics XL-MCL Flow Cytometer (Beckman Coulter, Fullerton, CA, USA). The flow cytometric results from Annexin V stained apoptotic cells were analyzed for statistical significance.

Matrigel invasion assay

We investigated the anti-tumor efficacy of LUT, SIL, or their combination in inhibiting the invasive ability of glioblastoma U87MG and T98G cells using the matrigel invasion assay. Transwell inserts (12-well, Corning Life Sciences, Corning, NY, USA) were coated with 200 µl of matrigel (BD Biosciences, San Jose, CA) to a final concentration of 1.0 mg/ml in ice-cold serum-free medium and allowed to dry at 37 °C for 4 h. At 24 h post-treatments, the control and treated cells were washed twice with serum-free medium, trypsinized, and 200 µl of cell suspension (2×10^5 cells) from each sample was added to each well in triplicate. After 48 h of incubation in presence of 5 % CO_2 at 37 °C, the membranes were collected and stained with HEMA 3 stain kit (Fisher Scientific, Kalamazoo, MI, USA). The cells that migrated to the undersurface of the membrane were examined under a light microscope, photographed, and counted in ten randomly selected microscopic fields.

In vitro network formation assay

This assay was performed to determine the anti-tumor actions of LUT, SIL, or their combination on the network formation of HME cells (Cascade Biologics, Portland, OR, USA) in co-culture with human glioblastoma U87MG or T98G cells. Glioblastoma cells (10^4 cells/well) were separately seeded into 4-well chamber slides and allowed to grow overnight. Similarly, HME cells were grown at 37 °C in HME medium (Cascade Biologics, Grand Island, NY, USA), supplemented with 15 mM HEPES, 2.5 mM L-glutamine, 10 % FBS (Mediatech, Atlanta Biologicals, Atlanta, GA, USA) and also 1 % penicillin and 1 % streptomycin (GIBCO/BRL, Grand Island, NY, USA) in a fully-humidified incubator containing 5 % CO_2. Next day, cells were treated with of LUT, SIL, or their combination for another 24 h and then co-cultured with HME cells (2×10^4 cells/well) in a 50:50 mixture of serum-free medium and HME medium. The co-cultures were terminated after 72 h, cells were fixed with 95 % ice-cold ethanol, and treated with the von Willebrand factor VIII antibody (Santa Cruz Biotechnology, Santa Cruz, CA, USA) followed by a biotinylated secondary antibody (Santa Cruz Biotechnology, Santa Cruz, CA, USA). After washings, the slides were further treated with horseradish peroxidase (HRP) conjugated streptavidin. The final stain was developed using 3 % 3-amino-9-ethylcarbazole in *N*,*N*-dimethylformamide. The cells were observed under the Olympus BX-53 microscope (Olympus America, Center Valley, PA, USA) and photographed. Quantitative analysis of the network formation was performed using Image-Pro Discovery software (Media Cybernetics, Silver Spring, MD, USA).

Cell migration from spheroids

Cell migration assay was performed to determine the anti-tumor effect of LUT, SIL, or their combination on cell migration from spheroids. To make the spheroids, glioblastoma U87MG and T98G cells were stably transfected with a red fluorescent protein following the manufacturer's protocol (Clontech, Mountain View, CA, USA), and treated with LUT, SIL, or their combination for 24 h. Cells were then washed thrice with HBSS (GIBCO/BRL, Grand Island, NY, USA), collected following centrifugation, counted, and seeded (5×10^4 cells/well) into 96-well low attachment culture plates (Corning Life Sciences, Corning, NY, USA) coated with 1 % agarose. Cells were incubated overnight in presence of 5 % CO_2 at 37 °C with constant shaking at 75 rpm to allow uniform formation of spheroids, which were then transferred to the center of wells of a 24-well culture plate and incubated in presence of 5 % CO_2 at 37 °C for 24 h. The migration of cells from the spheroids was examined under the Olympus BX-53 microscope (Olympus America Center Valley, PA, USA) and photographed. The percentage of migration of glioblastoma U87MG and T98G cells from the center of

the spheroid to the monolayer was calculated using a microscope calibrated with a stage and ocular micrometer and used as an index of cell migration. The data were presented as mean ± standard error of mean (SEM) of six independent experiments and compared with the control mean values.

Flow cytometric analysis of the acridine AO stained glioblastoma cells to quantify autophagic population

Autophagy plays a significant role in all cancers including glioblastoma by recycling of building blocks for promoting cell survival and growth of the established tumors. As a result of rapid cell proliferation in tumor cells, autophagy is highly upregulated in response to enhanced cellular stress and metabolic demands. Thus, autophagy induction augments cell survival by sustaining energy balance that helps tumor growth and chemotherapy resistance. In our study, we used RAPA pre-treated glioblastoma cells to observe the efficacy of LUT and SIL for inhibition of autophagy and enhancement of tumor cell death by induction of apoptosis. Formation of acidic vesicular organelles (AVO) is a characteristic feature of autophagic cells. Thus, we performed AO staining to detect and quantify the AVO by flow cytometry. Briefly, glioblastoma cells were pre-treated with 200 nM RAPA (an inducer of autophagy) for 24 h and then treated with LUT, SIL, or their combination for another 24 h followed by incubation with AO (1 μg/ml) for 15 min for staining. Then, flow cytometry was performed using AO stained glioblastoma cells. In flow cytometric analysis of the AO stained cells, cytoplasm and nucleolus in non-autophagic cells showed green fluorescence at FL-1 channel (500–550 nm) whereas AVO in autophagic cells (quadrant A1) showed bright red fluorescence at FL-3 channel (650 nm). Higher intensity of red fluorescence indicated larger number of AVO in autophagic cells. Therefore, amount of AVO in autophagic cells was quantified on the basis of the intensity of red fluorescence.

Protein extraction and Western blotting

Tumor cells or tissues from all treatment groups were homogenized in lysis buffer to make lysates for extraction of proteins. Protein concentrations were determined after staining the samples with Coomassie Plus protein reagent (Pierce Biotechnology, Rockford, IL, USA) using modified Bradford method. Then, protein samples were resolved by sodium dodecyl sulfate–polyacrylamide gel electrophoresis (SDS-PAGE) for Western blotting, as we previously described [28], using primary IgG antibodies against β-actin, LC3B, Beclin-1, PKCα, XIAP, iNOS, caspase-8, Bax, Bcl-2, caspase-9, and caspase-3 (Santa Cruz Biotechnology, Santa Cruz, CA, USA). The HRP conjugated goat anti-rabbit secondary IgG antibody (Santa Cruz Biotechnology, Santa Cruz, CA, USA) was used to detect primary IgG antibody. Western blots were incubated with enhanced chemiluminescence (ECL) reagents and exposed to X-OMAT AR films for autoradiography. Autoradiograms were scanned using the Epson Perfection V500 Photo Scanner.

Reverse transcription (RT) and quantification of pre-miRs by real-time qRT-PCR

At the end of all the desired treatments as described above, total RNA samples were extracted from glioblastoma U87MG and T98G cells using TRIZOL reagent following manufacturer's protocol (Invitrogen, Carlsbad, CA, USA). Three sets of primers against the tumor suppressor miRs (miR-7-1-3p, miR-9, and miR-181a) were designed from the primary precursor molecule sequences from the miRNA Database (miRDB). Custom synthesized primers were procured from Eurofins MWG Operon (Huntsville, AL, USA). The cDNA molecules were synthesized from total RNA samples using gene-specific primers following the procedure, as we reported previously [28, 29]. The gene-specific primers in the RT reaction included a mixture of 10 μM each of the antisense primers of all pre-miRs and U6 RNA. The levels of expression of the pre-miRs were determined using real-time qRT-PCR, as described previously [28, 29], with several modifications. All of the PCR reagents were used from the SYBR green core reagent kit (Applied Biosystems, Foster City, CA, USA). All pre-miRs and U6 RNA were assayed in duplicate in the reaction plates. Real-time PCR was performed on an Applied Biosystems 7900HT real-time qRT-PCR instrument. PCR was performed for 15 s at 95 °C and 1 min at 60 °C for 40 cycles followed by the thermal denaturation. The expression of each miR relative to U6 RNA was determined using the $2^{-\Delta CT}$ method. To simplify the presentation of the data, the relative expression values were multiplied by 10^2.

Development of glioblastoma xenografts in nude mice and drug treatments

Our animal studies were conducted strictly following the 'Guide for the Care and Use of Laboratory Animals' of the National Institutes of Health (NIH) and also approved by the Institutional Animal Care and Use Committee (IACUC) of the University of South Carolina (USC, Columbia, SC, USA). Anesthesia condition was maintained during all surgical procedures to minimize suffering of animals. Six-week-old female athymic (nu/nu) mice were obtained from Charles River Laboratories (Wilmington, MA, USA) and used for the development of tumors. Mice were injected subcutaneously (SC) with exponentially growing

glioblastoma U87MG or T98G cells (5×10^6) in 100 µl of a (1:1) mixture of 1xDMEM and matrigel (BD Biosciences, CA, USA) for development of tumors, as we described previously [30]. Treatments were started when tumors reached around 10 mm in diameter after 7 days. After 7 days of tumor inoculation, animals were daily pre-treated with RAPA (2 mg/kg body weight/day) for 7 days. One untreated control (CTL) group was kept in each set of experiments. We purchased miR-7-1-3p and anti-miR-7-1-3p mimics from Dharmacon (Chicago, IL, USA). After 7 days of RAPA pre-treatment, animals were randomly divided into 8 separate experimental groups (RAPA, RAPA + anti-miR-7-1-3p, RAPA + miR-7-1-3p, RAPA + LUT, RAPA + SIL, RAPA + miR-7-1-3p + LUT, RAPA + miR-7-1-3p + SIL, and RAPA + miR-7-1-3p + LUT + SIL). We used 6 mice in each treatment group. An equal volume of either anti-miR-7-1-3p or miR-7-1-3p and atelocollagen (0.1 % in PBS, pH 7.4) [31] were mixed for 1 h at 4 °C. Finally, an amount of 50 µg of anti-miR-7-1-3p or miR-7-1-3p in 200 µl of 0.05 % atelocollagen was injected into a mouse tail vein on alternate day for 7 days. Similarly, after 7 days of RAPA pre-treatment, mice were orally gavaged for 7 days with either LUT (10 mg/kg/day), or SIL (200 mg/kg/day), or their combination using a blunt-tipped 20-gauge 1.5 needle (Popper and Sons, New Hyde Park, NY, USA). After all miR and drug treatments for 7 days, mice were sacrificed under anesthesia, glioblastoma xenografts were surgically removed from the mice, and tumor volume was calculated using the formula: $V = \pi/6 \times$ larger diameter $\times$ (smaller diameter)^2 to assess regression of the tumor. We determined volume of each tumor to assess its regression due to a treatment.

Histopathological changes in tumors after the treatments

The RAPA pre-treated animals were treated with different therapeutic agents for a total of 7 days as described above and at the end of all treatments all animals were sacrificed under anesthesia. Then, tumors were surgically removed and divided into two halves. One half of the tumor was quickly frozen in liquid nitrogen and stored at −80 °C for subsequent use. Another half of the tumor was quickly frozen (−70 °C) in Optima Cutting Temperature (OCT) media (Fisher Scientific, Suwanee, GA, USA) for cutting 5 µm sections of tumor in OCT with a cryostat (Leica, Deerfield, IL, USA). Then, histopathological changes in the tumor sections were examined under the light microscopy after conventional H&E staining [30, 32].

Statistical analysis

The results from experiments were analyzed for statistical significance using Minitab® 16 statistical software (Minitab, State College, PA, USA). Data were expressed as mean ± SEM of separate experiments ($n \geq 3$) and compared by one-way analysis of variance (ANOVA) followed by the Fisher's post hoc test. Difference between a control (CTL) group and a treatment group was considered significant at $p < 0.05$.

Discussion

Our investigation demonstrated that the natural flavonoids LUT and SIL worked synergistically for inhibition of cell proliferation, invasion, and migration, and induction of apoptosis in human glioblastoma U87MG (wild-type p53) and T98G (mutant p53) cells. The anti-tumor activities of combination of LUT and SIL involved a significant increase in expression of the tumor suppressor miR-7-1-3p in both glioblastoma cells. Use of miRDB, an online resource for miR target prediction and functional annotations, suggested that miR-7-1-3p could target and degrade the mRNA of the anti-apoptotic XIAP gene in glioblastoma cells. Our in vivo studied indeed indicated that ectopic overexpression of miR-7-1-3p decreased expression of XIAP, augmented anti-tumor activities of LUT for inhibition of PKCα and autophagy, and also augmented anti-tumor activities of SIL for inhibition of iNOS and induction of both extrinsic and intrinsic pathways of apoptosis in the RAPA pre-treated glioblastoma U87MG (wild-type p53) and T98G (mutant p53) xenografts. Thus, overexpression of miR-7-1-3p enhanced anti-tumor activities of combination of LUT and SIL for controlling in vivo growth of human glioblastomas that harbored different p53 status.

We first demonstrated that treatment with combination of 20 µM LUT and 50 µM SIL worked synergistically and more effective than monotherapy with a conventional chemotherapeutic agent (10 µM BCNU or 100 µM TMZ) in causing significant decreases in cell viability in U87MG and T98G cells. Using CompuSyn software, we analyzed the results of residual cell viability to determine the synergistic growth inhibitory effects of 20 µM LUT and 50 µM SIL that showed CI values of 0.93 and 0.91, respectively, in U87MG and T98G cells. Therefore, we continued to use these concentrations of LUT and SIL for synergistic anti-tumor activities in all subsequent in vitro experiments. To identify the apoptotic mode of cell death, we performed in situ Wright staining and flow cytometric analysis. We observed more than 30 % apoptosis without any mechanical injury or necrosis following treatment with combination of LUT and SIL in glioblastoma cells. Then, we wanted to investigate if LUT and SIL possessed any anti-tumor activities in inhibiting invasion, network formation, and cell migration ability of glioblastoma U87MG and T98G cells. Our investigation showed that treatment with combination of LUT and SIL caused almost 90, 93,

and 92 % inhibition of invasion, network formation, and migration, respectively, in both glioblastoma cells. Our studies clearly demonstrated the anti-tumor activities of combination of LUT and SIL in inhibition of cell growth, induction of apoptosis, and inhibition of invasion, network formation, and migration.

Autophagy, which is a recycling of building blocks (e.g., carbohydrates, amino acids, nucleic acids) from the damaged cell components and organelles to promote proliferation in healthy cells, has recently emerged as an important survival mechanism is solid tumor cells that are under the stress conditions such a starvation. Use of RAPA in cell culture medium creates a condition of starvation leading to induction of autophagy in tumor cells [25, 26]. We wanted to investigate if treatment with combination of LUT and SIL could play a role in blocking a survival strategy like autophagy in the RAPA pre-treated glioblastoma cells. Our flow cytometric analysis of the AO stained RAPA pre-treated glioblastoma U87MG and T98G cells showed significant inhibition of autophagy in both cells following treatment with combination of LUT and SIL. Treatment with LUT alone or treatment with combination of LUT and SIL showed the most effective blockage of the autophagic survival process in glioblastoma cells. Our Western blotting showed alterations in the signaling molecules involved in autophagy and apoptosis in the RAPA pre-treated cells following treatments with LUT or/and SIL. Treatment with combination of LUT and SIL most effectively inhibited expression of PKCα, which could suppress RAPA-induced autophagy [33]. Suppression of autophagy was clearly evident in decreases in expression of Beclin-1, LC3B I, and LC3B II in both glioblastoma cell lines. Inhibition of PKCα is known to be associated with a down regulation of the anti-apoptotic protein XIAP leading to induction of apoptosis in tumor cells [34]. Our results from Western blotting also showed that treatment with SIL to some extent and combination of LUT and SIL to a greater extent inhibited expression of iNOS in the RAPA pre-treated both glioblastoma cells. Suppression of NO synthesis by iNOS could augment activation of caspase-8 and upregulation of p53 to trigger extrinsic and intrinsic apoptotic pathways, respectively, in glioblastoma cells. Indeed, treatment with combination of LUT and SIL induced extrinsic apoptotic pathway as evidenced from activation of caspase-8 and also intrinsic apoptotic pathway as evidenced from an increase in expression of Bax (pro-apoptotic protein) and decrease in expression of Bcl-2 (anti-apoptotic protein) leading to activation of caspase-9 and caspase-3 in the RAPA pre-treated both glioblastoma cells. These results clearly demonstrated the molecular mechanisms of combination of LUT and SIL for inhibition of autophagy and induction of apoptosis in glioblastoma cells.

Many recent investigations indicated the important roles of different tumor suppressor miRs in inhibiting cancer cell growth [35–37]. We performed an extensive search in the literature and miRDB (http://mirdb.org) for the tumor suppressor miRs in glioblastoma. Among them, we picked up miR-7-1-3p, miR-9, and miR-181a for examination of their levels of expression in glioblastoma cells in our current investigation. We observed the most significant increase in expression of miR-7-1-3p in the RAPA pre-treated glioblastoma U87MG and T98G cells following treatment with combination of LUT and SIL. Based on these results, we made a rationale that overexpression of miR-7-1-3p could further enhance the anti-tumor activities of combination of LUT and SIL for inhibition of autophagy and promotion of apoptosis in glioblastoma in vivo. Our in vivo studies indeed indicated that ectopic overexpression of miR-7-1-3p could further enhance the therapeutic efficacies of LUT and SIL in inhibiting tumor growth by inhibition of autophagy and induction of apoptosis in the RAPA pre-treated glioblastoma U87MG and T98G xenografts. Our miRDB search suggested that miR-7-1-3p could target and degrade the transcripts of XIAP, a potent anti-apoptotic protein. Our Western blotting suggested that overexpression of miR-7-1-3p was correlated with a decrease in XIAP, LUT treatment was involved with a drastic inhibition of PKCα and upregulation of the autophagy inhibitory markers like mTOR (an autophagy inhibitor) and p62 (an autophagy substrate), and SIL treatment was clearly correlated with down regulation of iNOS and activation of extrinsic and intrinsic caspase cascades for induction of apoptosis in the RAPA pre-treated glioblastoma xenografts. Based on these results, we schematically showed different molecular signaling pathways for inhibition of autophagy and induction of apoptosis in human glioblastoma in vivo (Fig. 9).

In conclusion, we demonstrated that combination of LUT and SIL could be a promising therapeutic strategy for inhibition of cell proliferation, migration, and invasion and induction of apoptosis in human glioblastoma U87MG and T98G cells. Although both LUT and SIL are involved in inhibition of survival pathways and induction of apoptosis, their target molecules in glioblastoma cells are different. Our results suggested that LUT and SIL exerted their anti-tumor activities by inhibiting expression PKCα and iNOS, respectively, in glioblastoma cells. Further, in vivo overexpression of miR-7-1-3p could target and degrade XIAP that otherwise played a crucial role in inhibition of caspases of the intrinsic pathway of apoptosis. Thus, overexpression of miR-7-1-3p followed by treatment with combination of LUT and SIL could provide a potential alternative therapeutic strategy for controlling growth of human glioblastomas irrespective of their p53 status. This new combination therapeutic strategy may circumvent current issues of chemotherapeutic drug resistance and adverse side effects in the treatment of human glioblastoma.

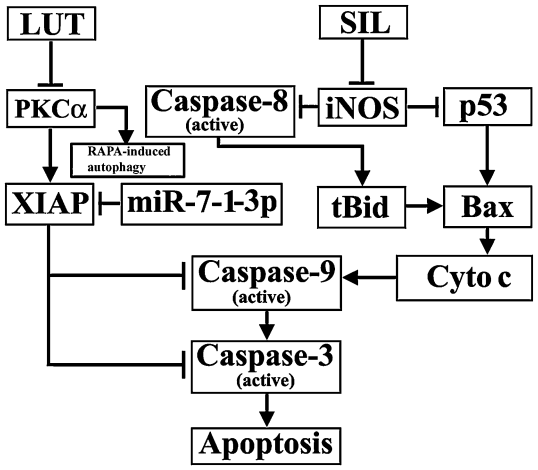

Fig. 9 Schematic presentation of the molecular signaling pathways to show inhibition of autophagy and induction of apoptosis in glioblastoma in vivo. Treatment of glioblastoma with LUT inhibited PKCα and thereby caused suppression of anti-apoptotic protein XIAP. Down regulation of PKCα also caused inhibition of RAPA-induced autophagy. Treatment of glioblastoma with SIL inhibited iNOS so as to result in upregulation of caspase-8 and p53 pathways that could trigger activation of both extrinsic and intrinsic pathways of apoptosis. An increase in Bax and decrease in Bcl-2 could alter mitochondrial permeability to release cytochrome c to trigger activation of intrinsic caspase cascade. Overexpression of miR-7-1-3p could also contribute to degradation of the anti-apoptotic XIAP so as to enhance induction of apoptosis. Thus, overexpression of miR-7-1-3p and combination of LUT and SIL could serve as a novel therapeutic strategy for inhibition of autophagy and induction of apoptosis in human glioblastoma in vivo

Acknowledgments This work was supported in part by the awards from the Research Development Fund (University of South Carolina School of Medicine, Columbia, SC, USA), the United Soybean Board (USB, Chesterfield, MO, USA), and the Spinal Cord Injury Research Fund (SCIRF-2015-I-01, Columbia, SC, USA).

Compliance with Ethical Standards

Conflict of interest The authors declare no conflict of interest

References

1. Ohgaki H, Kleihues P (2005) Population-based studies on incidence, survival rates, and genetic alterations in astrocytic and oligodendroglial gliomas. J Neuropathol Exp Neurol 64:479–489
2. Ravishankar D, Rajora AK, Greco F, Osborn HM (2013) Flavonoids as prospective compounds for anti-cancer therapy. Int J Biochem Cell Biol 45:2821–2831
3. Lin Y, Shi R, Wang X, Shen HM (2008) Luteolin, a flavonoid with potential for cancer prevention and therapy. Curr Cancer Drug Targets 8:634–646
4. Shimoi K, Okada H, Furugori M, Goda T, Takase S, Suzuki M, Hara Y, Yamamoto H, Kinae N (1998) Intestinal absorption of luteolin and luteolin 7-O-beta-glucoside in rats and humans. FEBS Lett 438:220–224
5. Wruck CJ, Claussen M, Fuhrmann G, Romer L, Schulz A, Pufe T, Waetzig V, Peipp M, Herdegen T, Gotz ME (2007) Luteolin protects rat PC12 and C6 cells against MPP^+ induced toxicity via an ERK dependent Keap1-Nrf2-ARE pathway. J Neural Transm Suppl 72:57–67
6. Lamy S, Moldovan PL, Ben Saad A, Annabi B (2015) Biphasic effects of luteolin on interleukin-1β-induced cyclooxygenase-2 expression in glioblastoma cells. Biochim Biophys Acta 1853:126–135
7. Cheng WY, Chiao MT, Liang YJ, Yang YC, Shen CC, Yang CY (2013) Luteolin inhibits migration of human glioblastoma U-87 MG and T98G cells through downregulation of Cdc42 expression and PI3 K/AKT activity. Mol Biol Rep 40:5315–5326
8. Shi RX, Ong CN, Shen HM (2005) Protein kinase C inhibition and X-linked inhibitor of apoptosis protein degradation contribute to the sensitization effect of luteolin on tumor necrosis factor-related apoptosis-inducing ligand-induced apoptosis in cancer cells. Cancer Res 65:7815–7823
9. Selvendiran K, Koga H, Ueno T, Yoshida T, Maeyama M, Torimura T, Yano H, Kojiro M, Sata M (2006) Luteolin promotes degradation in signal transducer and activator of transcription 3 in human hepatoma cells: an implication for the antitumor potential of flavonoids. Cancer Res 66:4826–4834
10. Chiang CT, Way TD, Lin JK (2007) Sensitizing HER2-overexpressing cancer cells to luteolin-induced apoptosis through suppressing p21(WAF1/CIP1) expression with rapamycin. Mol Cancer Ther 6:2127–2138
11. Son YG, Kim EH, Kim JY, Kim SU, Kwon TK, Yoon A, Yun CO, Choi KS (2007) Silibinin sensitizes human glioma cells to TRAIL-mediated apoptosis via DR5 up-regulation and down-regulation of c-FLIP and survivin. Cancer Res 67:8274–8284
12. Tyagi A, Agarwal C, Harrison G, Glode LM, Agarwal R (2004) Silibinin causes cell cycle arrest and apoptosis in human bladder transitional cell carcinoma cells by regulating CDKI–CDK–cyclin cascade, and caspase 3 and PARP cleavages. Carcinogenesis 25:1711–1720
13. Yang SH, Lin JK, Chen WS, Chiu JH (2003) Anti-angiogenic effect of silymarin on colon cancer lovo cell line. J Surg Res 113:133–138
14. Chu S, Chiou H, Chen P, Yang S, Hsieh Y (2004) Silibinin inhibits the invasion of human lung cancer cells via decreased productions of urokinase-plasminogen activator and matrix metalloproteinase-2. Mol Carcinog 40:143–149
15. Katiyar SK, Korman NJ, Mukhtar H, Agarwal R (1997) Protective effects of silymarin against photocarcinogenesis in a mouse skin model. J Natl Cancer Inst 89:556–566
16. Singh RP, Agarwal R (2004) Prostate cancer prevention by silibinin. Curr Cancer Drug Targets 4:1–11
17. Momeny M, Khorramizadeh MR, Ghaffari SH, Yousefi M, Yekaninejad MS, Esmaeili R, Jahanshiri Z, Nooridaloii MR (2008) Effects of silibinin on cell growth and invasive properties of a human hepatocellular carcinoma cell line, HepG-2, through inhibition of extracellular signal-regulated kinase 1/2 phosphorylation. Euro J Pharmacol 591:13–20
18. Singh RP, Deep G, Chittezhath M, Kaur M, Dwyer-Nield LD, Malkinson AM, Agarwal R (2006) Effect of silibinin on the growth and progression of primary lung tumors in mice. J Natl Cancer Inst 98:846–855
19. Tyagi A, Singh RP, Agarwal C, Agarwal R (2006) Silibinin activates p53-caspase 2 pathway and causes caspase-mediated cleavage of Cip1/p21 in apoptosis induction in bladder transitional-cell papilloma RT4 cells: evidence for a regulatory loop between p53 and caspase 2. Carcinogenesis 27:2269–2280
20. Reddy SD, Ohshiro K, Rayala SK, Kumar R (2008) microRNA-7, a homeobox D10 target, inhibits p21-activated kinase 1 and regulates its functions. Cancer Res 68:8195–8200
21. Lai EC, Tam B, Rubin GM (2005) Pervasive regulation of Drosophila Notch target genes by GY-box-, Brd-box-, and K-box-class microRNAs. Genes Dev 19:1067–1080

22. Li X, Carthew RW (2005) A microRNA mediates EGF receptor signaling and promotes photoreceptor differentiation in the Drosophila eye. Cell 123:1267–1277
23. Babae N, Bourajjaj M, Liu Y, Van Beijnum JR, Cerisoli F, Scaria PV, Verheul M, Van Berkel MP, Pieters EH, Van Haastert RJ, Yousefi A, Mastrobattista E, Storm G, Berezikov E, Cuppen E, Woodle M, Schaapveld RQ, Prevost GP, Griffioen AW, Van Noort PI, Schiffelers RM (2014) Systemic miRNA-7 delivery inhibits tumor angiogenesis and growth in murine xenograft glioblastoma. Oncotarget 5:6687–6700
24. Kefas B, Godlewski J, Comeau L, Li Y, Abounader R, Hawkinson M, Lee J, Fine H, Chiocca EA, Lawler S, Purow B (2008) microRNA-7 inhibits the epidermal growth factor receptor and the Akt pathway and is down-regulated in glioblastoma. Cancer Res 68:3566–3572
25. Noda T, Ohsumi Y (1998) TOR, a phosphatidylinositol kinase homologue, controls autophagy in yeast. J Biol Chem 273:3963–3966
26. Wullschleger S, Loewith R, Hall MN (2006) TOR signaling in growth and metabolism. Cell 124:471–484
27. Chou TC (2006) Theoretical basis, experimental design, and computerized simulation of synergism and antagonism in drug combination studies. Pharmacol Rev 58:621–681
28. Chakrabarti M, Khandkar M, Banik NL, Ray SK (2012) Alterations in expression of specific microRNAs by combination of 4-HPR and EGCG inhibited growth of human malignant neuroblastoma cells. Brain Res 1454:1–13
29. Chakrabarti M, Ai W, Banik NL, Ray SK (2013) Overexpression of miR-7-1 increases efficacy of green tea polyphenols for induction of apoptosis in human malignant neuroblastoma SH-SY5Y and SK-N-DZ cells. Neurochem Res 38:420–432
30. Chakrabarti M, Banik NL, Ray SK (2013) Photofrin based photodynamic therapy and miR-99a transfection inhibited FGFR3 and PI3 K/Akt signaling mechanisms to control growth of human glioblastoma in vitro and in vivo. PLoS One 8:e55652
31. Takeshita F, Patrawala L, Osaki M, Takahashi RU, Yamamoto Y, Kosaka N, Kawamata M, Kelnar K, Bader AG, Brown D, Ochiya T (2010) Systemic delivery of synthetic microRNA-16 inhibits the growth of metastatic prostate tumors via downregulation of multiple cell-cycle genes. Mol Ther 18:181–187
32. Chakrabarti M, Banik NL, Ray SK (2013) miR-138 overexpression is more powerful than hTERT knockdown to potentiate apigenin for apoptosis in neuroblastoma in vitro and in vivo. Exp Cell Res 319:1575–1585
33. Tan SH, Shui G, Zhou J, Li JJ, Bay BH, Wenk MR, Shen HM (2012) Induction of autophagy by palmitic acid via protein kinase C-mediated signaling pathway independent of mTOR (mammalian target of rapamycin). J Biol Chem 287:14364–14376
34. Kang JH, Asai D, Yamada S, Toita R, Oishi J, Mori T, Niidome T, Katayama Y (2008) A short peptide is a protein kinase C (PKC)α-specific substrate. Proteomics 8:2006–2011
35. Chen G, Zhu W, Shi D, Lv L, Zhang C, Liu P, Hu W (2010) microRNA-181a sensitizes human malignant glioma U87MG cells to radiation by targeting Bcl-2. Oncol Rep 23:997–1003
36. Fang Y, Xue JL, Shen Q, Chen J, Tian L (2012) microRNA-7 inhibits tumor growth and metastasis by targeting the phosphoinositide 3-kinase/Akt pathway in hepatocellular carcinoma. Hepatology 55:1852–1862
37. Wang LQ, Kwong YL, Kho CS, Wong KF, Wong KY, Ferracin M, Calin GA, Chim CS (2013) Epigenetic inactivation of miR-9 family microRNAs in chronic lymphocytic leukemia—implications on constitutive activation of NF-κB pathway. Mol Cancer 12:173